ADVANCES IN ATMOSPHERIC SCIENCES, VOL. 29, NO. 3, 2012, 471–483

The East Pacific Wavetrain: Its Variability and Impact on the Atmospheric Circulation in the Boreal Winter

ZHOU Putian[1] (周普天), SUO Lingling[1,2,3] (所玲玲),
YUAN Jiacan[1] (袁嘉灿), and TAN Benkui*[1] (谭本馗)

[1] *Department of Atmospheric and Oceanic Sciences, School of Physics, Peking University, Beijing* 100871

[2] *Nansen Environmental and Remote Sensing Center, Bergen, Norway*

[3] *Bjerknes Center for Climate Research, Bergen, Norway*

(Received 12 September 2010; revised 7 August 2011)

ABSTRACT

The East Pacific wavetrain (EPW) refers to here the intense stationary wave activity detected in the troposphere over the East Pacific and North America in 45 northern winters from 1958 to 2002. The EPW is generated in the lower troposphere over the East Pacific, propagating predominantly eastward into North America and slightly upward then eventually into the stratosphere. The intensity of the EPW varies from year to year and exhibits apparent decadal variability. For the period 1958–1964, the EPW was in its second maximum, and it was weakest for the period 1965–1975, then it was strongest for the period 1976–1987. After 1987, the EPW weakened again.

The intensity and position of the members (i.e., the Aleutian low, the North American trough, and the North American ridge) of the EPW oscillate from time to time. For an active EPW versus a weak EPW, the Aleutian low deepens abnormally and shifts its center from the west to the east of the date line, in the middle and upper troposphere the East Asian trough extends eastward, and the Canadian ridge intensifies at the same time. The opposite is true for a weak EPW. Even in the lower stratosphere, significant changes in the stationary wave pattern are also observed.

Interestingly the spatial variability of the EPW assumes a Pacific–North American (PNA)-like teleconnection pattern. It is likely that the PNA low-frequency oscillation is a reflection of the oscillations of intensity and position of the members of the EPW in horizontal direction.

Key words: East Pacific wavetrain, stationary waves, vertical propagation

Citation: Zhou, P. T., L. L. Suo, J. C. Yuan, and B. K. Tan, 2012: The East Pacific wavetrain: Its variability and impact on the atmospheric circulation in the boreal winter. *Adv. Atmos. Sci.*, **29**(3), 471–483, doi: 10.1007/s00376-011-0216-3.

1. Introduction

The stationary waves in the atmosphere usually refer to the semi-permanent atmospheric centers of action such as the Siberian high, the Aleutian low, and the Icelandic low in the lower troposphere of the northern winter. These waves are generally believed to be generated in the troposphere by topographic and thermal forcing (Charney and Eliassen, 1949; Smagorinsky, 1953), then they propagate away from the wave sources horizontally (Held, 1983; Held et al., 2002) and vertically upward into the stratosphere under some favorable conditions (Charney and Drazin, 1961; Dickinson, 1968; Matsuno, 1970). So the stationary waves have much to do with the anomalies of the atmospheric circulation and climate far away from the wave sources (see, e.g., Matsuno, 1971; Andrews et al., 1987; Haynes, 2005).

For many years the role of the stationary waves in the stratosphere–troposphere dynamical coupling has been considered a one-way effect of the troposphere on the stratosphere. But recently, more and

*Corresponding author: TAN Benkui, bktan@pku.edu.cn

more observational and modeling evidence shows that the stratosphere does not always play a passive role and that the changes in the stratosphere may cause the changes in the troposphere. Dunkerton and Baldwin (1991), Baldwin and Dunkerton (2001) and Wallace and Thompson (2002) found that the atmospheric anomalies associated with the Arctic oscillation (AO) or ozone depletion can first appear in the stratosphere then propagate downward into the troposphere and exert feedbacks on the troposphere's weather and climate. Although the mechanism behind the stratosphere's affect on the troposphere is still not completely clear, it is believed that the stationary wave propagation somehow plays an important role. One possible approach considers the stratospheric modulation on the stationary wave propagation and the wave-mean flow interaction in the troposphere and stratosphere (Hartmann et al., 2000; Limpasuvan and Hartmann, 2000; Ambaum and Hoskins, 2002; Black, 2002). Particularly, downward reflection from the stratosphere and the associated tropospheric circulation changes have been observed (Kuroda and Kodera, 1999; Perlwitz and Graf, 2001; Perlwitz and Harnik, 2004; Kodera et al., 2008).

In most of the literature the propagation of the stationary waves and their interactions with mean flow have been diagnosed mainly via the Eliassen-Palm (E-P) flux (Andrews and McIntyre, 1976). The waves propagate mainly along the two waveguides, that is, the polar waveguide and equatorial waveguide (Huang and Gambo, 1982, 1983). The variability of the two waveguides has much to do with the atmospheric variability, such as the Arctic oscillation/annual modes (Hartmann et al., 2000; Limpasuvan and Hartmann, 2000; Chen et al., 2003). Although the E-P flux has been widely used and much progress has been made, its drawbacks are also obvious: (1) it can reveal only the two-dimensional propagation characteristics in the (y, z) plane, and (2) the details of the zonal propagation remain elusive in spite of the fact that the zonal propagation is dominant and longitudinally dependent. To overcome this drawback, Plumb (1985) developed a new formula suitable for the three-dimensional stationary waves and applied the formula to the northern winters. Plumb's work clearly reveals the wave sources and wave paths (see Plumb, 1985, and section 3 for more details).

In this study we focused on the northern winter stationary wave activity over the East Pacific and North America. Our work was actually motivated by Randel and Williamson (1990), Yang and Gutowski (1994), and Suo (2008), who detected an extensive stationary wave activity over the East Pacific–North America sector in northern winters with the same or different data sets for different time periods, which was very weak in Plumb (1985). What causes the difference between Plumb (1985) and his followers? As pointed out in Yang and Gutowski (1994), the new wave activity may represent changes in "stationary waves" from one decade to another, or it may be the result of the many changes in the NMC reanalysis schemes over the period 1965–1990. This is an interesting problem that has not yet attracted attention. This study aimed to answer this question. Our results show that this difference does represent a variability of the stationary waves over East Pacific and North America. The three-dimensional characteristics of the wave activity, its influence on the atmospheric circulations and possible connection with the well known Pacific-North America (PNA) teleconnection pattern (Wallace and Gutzler, 1981) was investigated, and our results are presented here.

The paper is organized as follows. The next section describes the data and methods used. In section 3 the three-dimensional propagation features of the stationary waves revealed in the wave fluxes and the temporal variability over the East Pacific–North America are examined. Then the spatial variability of the East Pacific wavetrain (EPW) in the geopotential height and temperature fields and its relation to the PNA pattern are investigated in sections 4 and 5, respectively. Finally, a brief summary and conclusions are given in section 6.

2. Data and methods

The data used in this study are the monthly mean gridded data of the ERA-40 reanalysis data set from the European Center for Medium-Range Weather Forecasting (ECMWF) reanalysis project (Uppala et al., 2005). The data covered the period from December 1957 to February 2002, and only northern winter months (December–February or DJF) were considered.

To reveal the three-dimensional propagation features of the waves, Eq. (5.7) in Plumb (1985), as in Randel and Williamson (1990), Yang and Gutowski (1994) and Suo (2008), was used to calculate the wave fluxes:

$$\boldsymbol{F}_{\mathrm{s}} = p\cos\varphi \begin{bmatrix} \dfrac{1}{2\mathrm{a}^2\cos^2\varphi}\left[\left(\dfrac{\partial\psi'}{\partial\lambda}\right)^2 - \psi'\dfrac{\partial^2\psi'}{\partial\lambda^2}\right] \\ \dfrac{1}{2\mathrm{a}^2\cos\varphi}\left(\dfrac{\partial\psi'}{\partial\lambda}\dfrac{\partial\psi'}{\partial\varphi} - \psi'\dfrac{\partial^2\psi'}{\partial\lambda\partial\varphi}\right) \\ \dfrac{2\Omega^2\sin^2\varphi}{N^2 a\cos\varphi}\left(\dfrac{\partial\psi'}{\partial\lambda}\dfrac{\partial\psi'}{\partial z} - \psi'\dfrac{\partial^2\psi'}{\partial\lambda\partial z}\right) \end{bmatrix}, \tag{1}$$

where the vector $\boldsymbol{F}_s$ is the three-dimensional wave flux of the stationary waves (the Plumb flux, hereafter), which is derived under the quasi-geostrophic approximation. In this equation, p = pressure/1000 hPa, $z = -H \ln p$ and H is a constant scaleheight. a, Ω, ϕ, λ represent the Earth's radius, the Earth's rotation rate, latitude and longitude, respectively. ψ' is the small perturbation of the streamfunction to its zonal mean. N is the buoyancy frequency. The Plumb fluxes are parallel to the local group velocities and thus provide a good indicator of the wave propagation. The northward and upward components of the Plumb fluxes reduce to the E-P fluxes when they are integrated along the whole latitude circle (Plumb, 1985).

According to the literature, two methods are usually used to obtain the climatology of the wave fluxes for periods such as the 45 winters from 1958 to 2002. The first approach is to calculate the climatology of the stationary flow at each level by averaging the geopotential height at that level for the total 45 winters, then to obtain the stationary waves by simply removing the corresponding zonal mean of the geopotential height, and finally to obtain the climatology of the Plumb fluxes by applying the Plumb's formula to the stationary waves. The second way to get the climatology of the Plumb fluxes for these 45 winters is to compute the stationary flow of each winter at each level by averaging the geopotential height of the three winter months at each level, then to obtain the stationary waves of a winter by removing the corresponding zonal mean of the geopotential height, and then to apply Plumb's formula to the winter mean stationary waves, and finally to add up the winter mean Plumb fluxes for the total 45 winters to give the overall climatology. Some differences were expected between these two methods because the Plumb's formula is nonlinear for the perturbations of the geopotential height. However, no apparent differences were actually found, so we report the results obtained using the second method. Similarly, the mean distributions of the Plumb fluxes for other shorter periods of time and the composites of the Plumb fluxes for the active EPW and the weak EPW were also calculated with the second approach.

As in Suo (2008), the domain considered here was extended from the troposphere into the stratosphere ranging vertically from 1000 hPa to 1 hPa, while in Plumb (1985), Randel and Williamson (1990), and Yang and Gutowski (1994) only the troposphere was taken into consideration. However, we report only the results up to 50 hPa because the results did not reach the 5% significance level above 50 hPa. As a consequence, our results shed some light on the propagating characteristics of the stationary waves in the lower stratosphere and their role in stratosphere–troposphere coupling.

3. Three-dimensional features of the EPW and its temporal variability

This section discusses the propagation features of the northern winter stationary waves revealed by the Plumb flux. Figure 1a shows the climatological mean of the northern winter stationary wave fluxes at 500 hPa for the period 1958–2002, in which the arrows and contours represent the horizontal and vertical components of the fluxes, respectively. As in Plumb (1985), two intensive centers of wave activity are evident over the East Asia–West Pacific and the North Atlantic; they are termed as the East Asia–West Pacific wavetrain and the North Atlantic wavetrain, respectively. Different from Plumb (1985), a new center of intensive wave activity, i.e., the EPW, can be clearly seen over the East Pacific and North America, whereas this feature is very weak in Plumb (1985, Fig. 4a).

These features can be seen in both the ECMWF and NCEP/NCAR reanalysis data sets with no significant difference, so it is reasonable to believe that the difference between our work and Plumb's was possibly caused by the differences of the time periods used instead of difference in the data sources. To make this clear, we examined the wave fluxes winter by winter and found that the magnitude of the EPW did vary from year to year. To better describe this variation, we defined an index as the volume-averaged winter-mean vertical stationary wave fluxes in the domain (30°–60°N, 170°–120°W; 925–500 hPa; the gray boxes in Fig. 1). The index thus defined was not very sensitive to the exact domain and was thus a good indicator of the strength of the EPW. Figure 2a shows the time series of the standardized index for the period 1958–2002. It is clear that the index varies from year to year and a variation on a decadal scale is also obvious. The index is in its second maximum from 1958 to 1964, in its weakest from 1965 to 1975 and reaches the maximum from 1976 to 1987. After 1987 it becomes weaker again.

The corresponding composites of the wave fluxes are in good agreement with the results based on the wave index. A weakest EPW is observed during 1965–1975 [Fig. 1c (this article); also Fig. 4a in Plumb, 1985], and an active EPW appears in 1976–1987 and in 1958–1964 [Fig. 1b, d (this article); also Fig. 18c in Randel and Williamson (1990) and Fig. 4 in Yang and Gutowski (1994)].

The abrupt change in the strength of the EPW around 1976–1977 may be a reflection of the abrupt climate shift that occurred in the North Pacific as detected in Trenberth and Hurrell (1994). As discussed

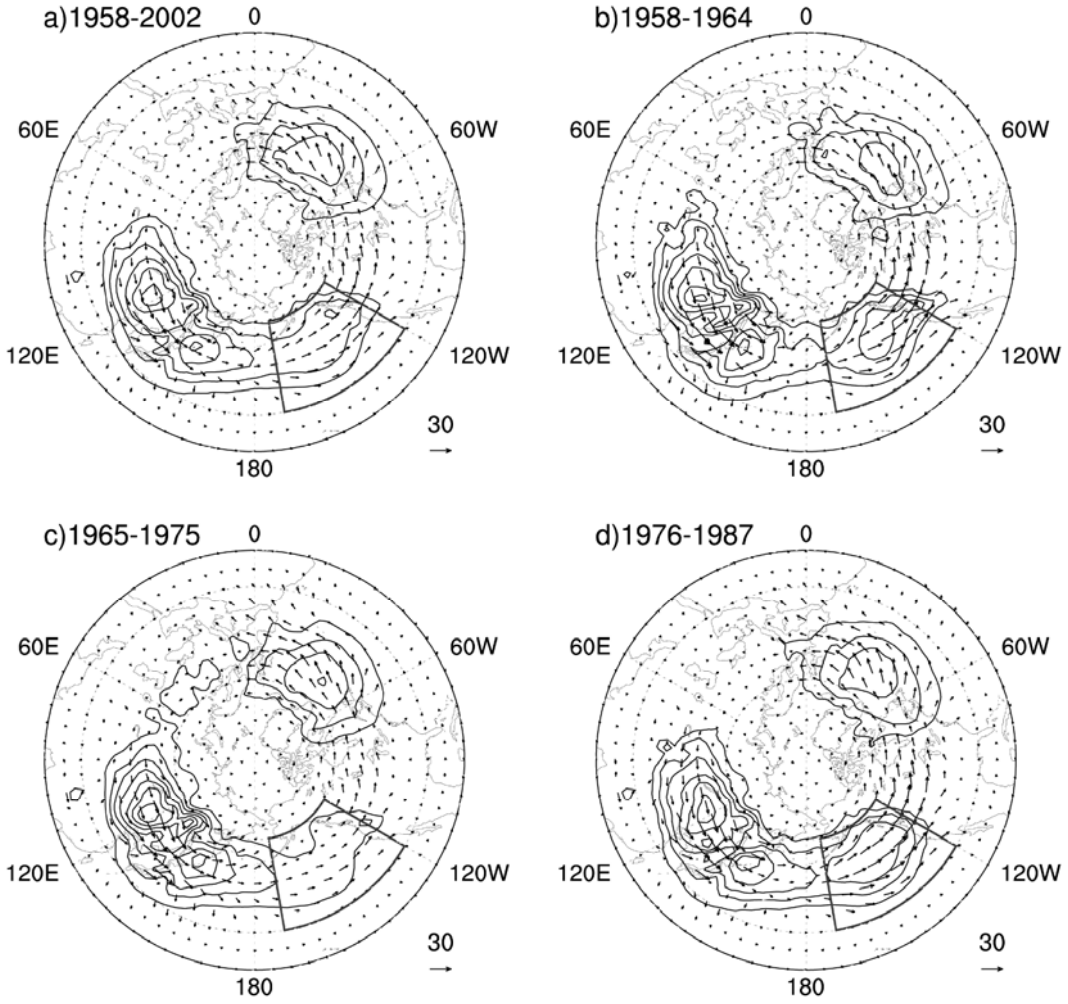

Fig. 1. Distribution of the northern winter stationary wave fluxes at 500 hPa for (a) 1958–2002; (b) 1958–1964; (c) 1965–1975 and (d) 1976–1987. Arrows: horizontal components and reference vectors are shown on the bottom right of each map. Contours: vertical components and positive contours are solid, zero lines and negative contours are not shown. Units: $m^2\ s^{-2}$. Contour interval: 0.05. Gray boxes represent the horizontal domain (30°–60°N, 170°–120°W) used to define the EPW index.

in section 4, the EPW is closely related with the PNA low frequency oscillation and the PNA also shows an abrupt phase shift around 1976/1977 (Namias et al., 1988; Nitta and Yamada, 1989).

Next we analyzed the three-dimensional propagation features of the EPW. To this end, we chose the active and weak EPW winters from the total 45 winters based on the standardized EPW index. A winter was labeled as "an active EPW winter" when the index of the winter was $\geqslant$1.0 and as "a weak EPW winter" when the index was $\leqslant -1.0$. Thus, we identified eight active EPW winters: 1961 (referring to Dec 1960, Jan 1961, Feb 1961, likewise throughout), 1963, 1970, 1977, 1981, 1983, 1986, and 2001. We identified seven weak EPW winters: 1965, 1966, 1969, 1971, 1972, 1982, and 1999.

Figure 3 shows the composites of the stationary wave fluxes at different levels from the troposphere to the lower stratosphere based on the active EPW winters and weak EPW winters, separately. The gray shadows in Fig. 3 show the areas where the vertical stationary fluxes are significantly different from their climatology at the 1% significance level. As can be seen from Fig. 3, the East Asia–West Pacific and North Atlantic wavetrains still dominated in the troposphere, though they were weaker for the weak EPW winters than for the active EPW winters. Starting from Mongolia, the East Asian–West Pacific wavetrain propagates upward and eastward, across East Asia and into the West Pacific where the wave fluxes bifurcate

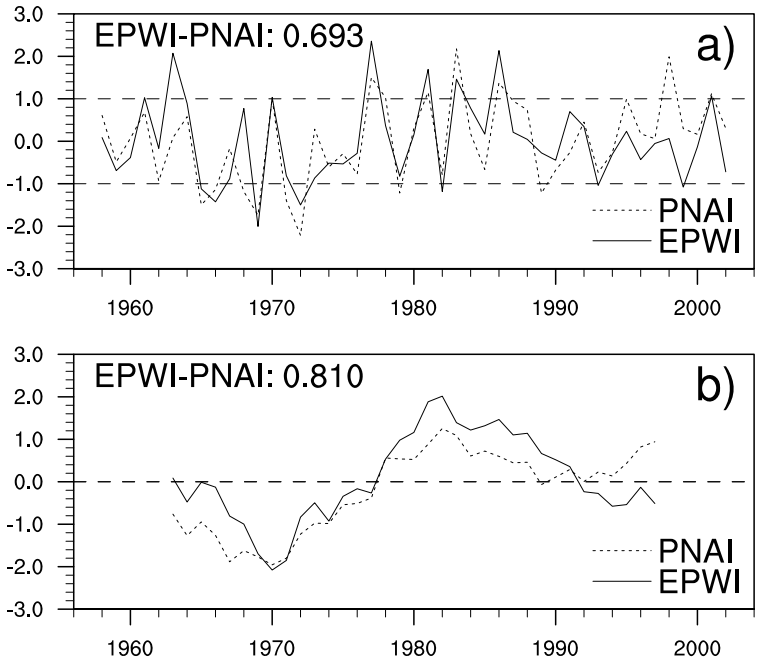

Fig. 2. Standardized time series of the EPW index (solid line) and the PNA index (dashed line) from 1958 to 2002 calculated with (a) winter mean index and (b) 11-year running mean index. The correlation coefficients between the EPW index and the PNA index are shown at the top left of each picture.

into two branches: the northern branch continues to propagate dominantly eastward, slightly poleward and upward, which enters the stratosphere finally while the southern branch propagates eastward, southward and upward to the top of the troposphere where the wave flux turns into the tropics. The North Atlantic wavetrain starts from the North America coast and propagates eastward and equatorward, spreading across the whole North Atlantic into the West Europe and northern Africa. The North Atlantic wave train also propagates upward, but its vertical propagation is confined within the troposphere.

From weak to active EPW winters, the EPW behaves quite differently: it disappears almost completely for weak EPW winters and becomes extremely active for active EPW winters. At this time it is even stronger than the North Atlantic wavetrain and almost as strong as the East Asia–West Pacific wavetrain (Figs. 3a, b). Starting from the central North Pacific, the horizontal wave fluxes of the EPW propagate predominantly eastward across the East Pacific and North America. There exists a clear boundary area with diminished horizontal wave fluxes at the central North Pacific region, which separates the East Asia–West Pacific wavetrain and the EPW well (Figs. 3a, b). So it is reasonable to consider the EPW as an independent wavetrain. The vertical wave fluxes, on the other hand, concentrate on the East Pacific, with positive signs all the way through the troposphere to the lower stratosphere (Figs. 3a–d), which means that the EPW is produced in the lower troposphere and propagates upward into the stratosphere. This is why it is known as the East Pacific wavetrain rather than the East Pacific–North America wavetrain.

In the lower stratosphere, there is an intense upward wave-flux center across East Asia and North Pacific, which is mainly due to the vertical propagation of the East Asia–West Pacific wavetrain (Figs. 3c, d, g, h). A small area of negative vertical wave fluxes over Canada can be seen, which is generally believed to be a result of the reflection of the East Asia–West Pacific wavetrain from a higher level of the stratosphere (Kodera et al., 2008). Obviously, this downward reflection is considerably weakened by the vertical propagation of the EPW. However, the area of negative wave fluxes does reach the 5% significance level.

4. Atmospheric circulation response

In the previous section the propagation features of the EPW revealed by the wave flux were discussed. In this section we examine the EPW features in the geopotential height and temperature fields, i.e., how the members of the stationary waves, such as the Aleu-

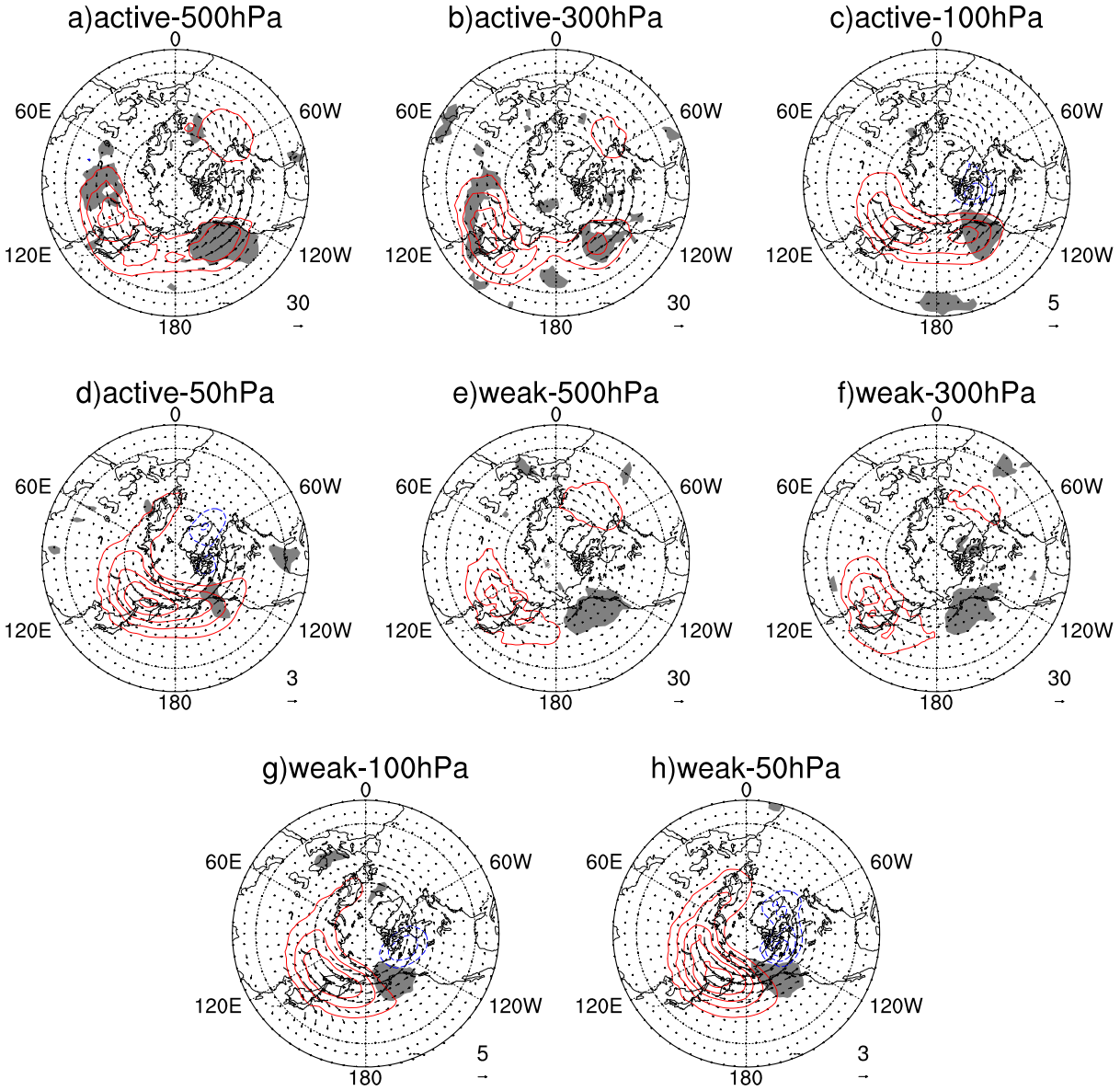

Fig. 3. Composites of the stationary wave fluxes at 500 hPa, 300 hPa, 100 hPa, and 50 hPa for the active EPW (a, b, c, d) and weak EPW (e, f, g, h). Arrows: horizontal components and reference vectors are shown on the bottom right of each map. Contours: vertical components and positive contours are in red and negative contours are in blue, zero lines are not shown. Units: $m^2\ s^{-2}$. Positive contour interval: 0.1 for (a) and (e); 0.05 for (b) and (f); 0.01 for (c) and (g); and 0.005 for (d) and (h); negative contour interval: 0.1 for (a) and (e); 0.05 for (b) and (f); 0.005 for (c) and (g); and 0.002 for (d) and (h). Gray shadows show the statistical significance at the 1% level.

tian low, the Asian trough, the American ridge, and the American trough, behave for the active EPW and the weak EPW. Figure 4 shows the composites of the stationary waves in geopotential height field for the active EPW and weak EPW separately. At the surface the Siberia high and Icelandic low change only slightly from the active EPW to the weak EPW, but the Aleutian low deepens abnormally and shifts its center from the west to the east of the date line for the active EPW versus the weak EPW (Fig. 4a). In the middle and upper troposphere, the East Asian trough extends eastward considerably for the active EPW and retreats backward for the weak EPW (Fig. 4b). The Canadian ridge also changes remarkably. It intensifies abnormally for the active EPW, and the opposite is true for the weak EPW. Over the North Atlantic

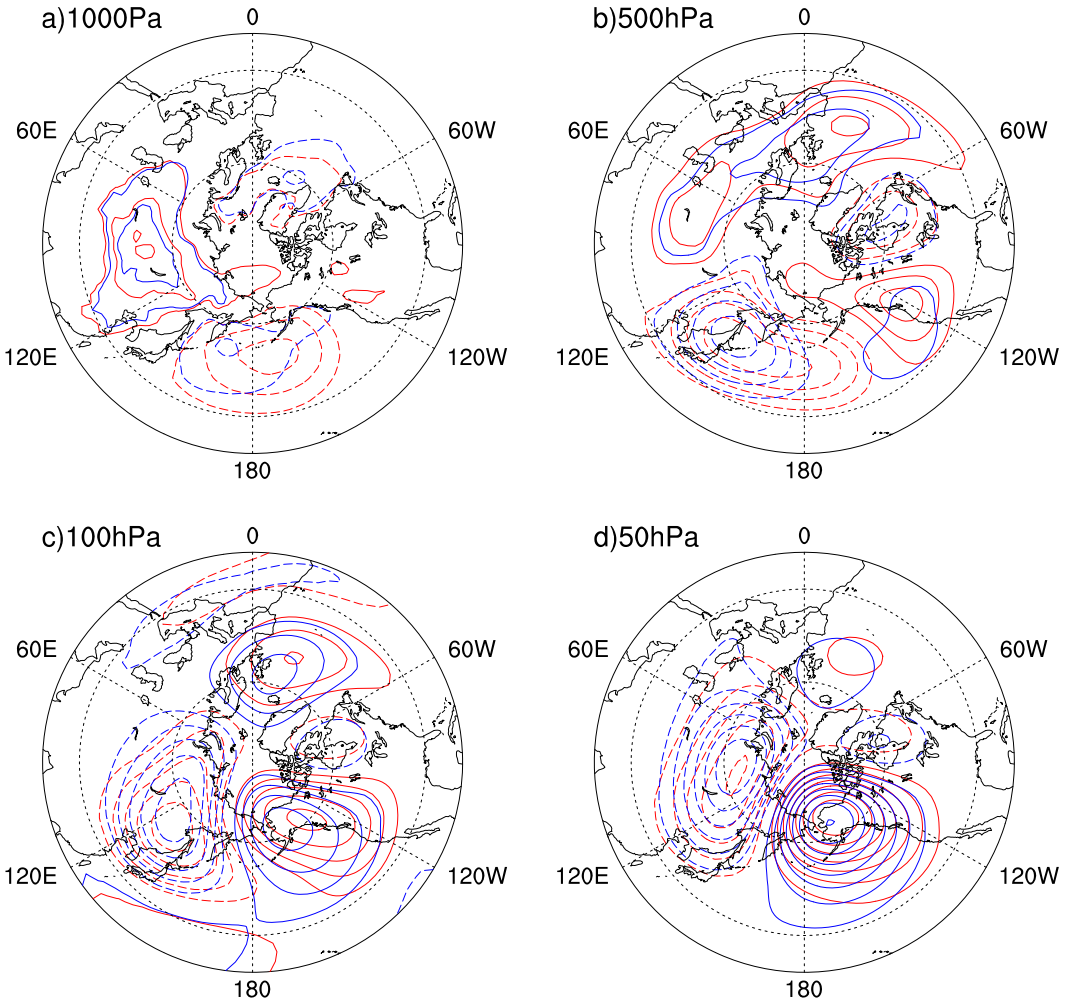

Fig. 4. Composites of the geopotential height of the stationary waves for the active EPW (red curves) and weak EPW (blue curves) at (a) 1000 hPa; (b) 500 hPa; (c) 100 hPa, and (d) 50 hPa. Units: $m^2\ s^{-2}$. Contour interval: 500. Solid and dashed lines represent positive and negative values, respectively; zero lines are not shown.

and the Eurasian continent, some notable variations can also be seen. The North Atlantic ridge intensifies slightly and shifts southwestward, while the European ridge intensifies slightly for the active EPW against the weak EPW. In the lower stratosphere at 100 hPa, the three centers of the stationary waves also show noticeable changes. The American high weakens and shifts westward, while the Atlantic high intensifies and shifts northeastward for the weak EPW versus the active EPW (Fig. 4c). At 50 hPa (Fig. 4d), the low over Eurasian deepens to some extent for the weak EPW versus the active EPW, and the high over North Pacific shifts slightly westward. The weak high over the North Atlantic and the weak low over North America also show some change in intensity and shape.

The variation of the spatial patterns of the EPW in the geopotential height and temperature fields can be shown more clearly in the difference maps between the composites of the active EPW and weak EPW (Fig. 5). Student's t-test was used to conduct the significance test of the difference in composite maps (including the composite maps described below, Figs. 5, 6, 7, 8). Interestingly and also unexpectedly, the anomalous geopotential height pattern over the North Pacific–North America sector assumes a PNA-like pattern. Over the North Atlantic–Eurasia continent sector, the geopotential height anomalies, which are much weaker than the PNA-like pattern, take a form of wavetrain with its three centers locating over North Atlantic, Scandinavia, and the Northern Eurasia continent, respectively, but not all of the anomalies reach the 5% significance level. The PNA-like pattern reaches its maximum amplitude around the upper troposphere and degrades into a dipole form in the lower tropo-

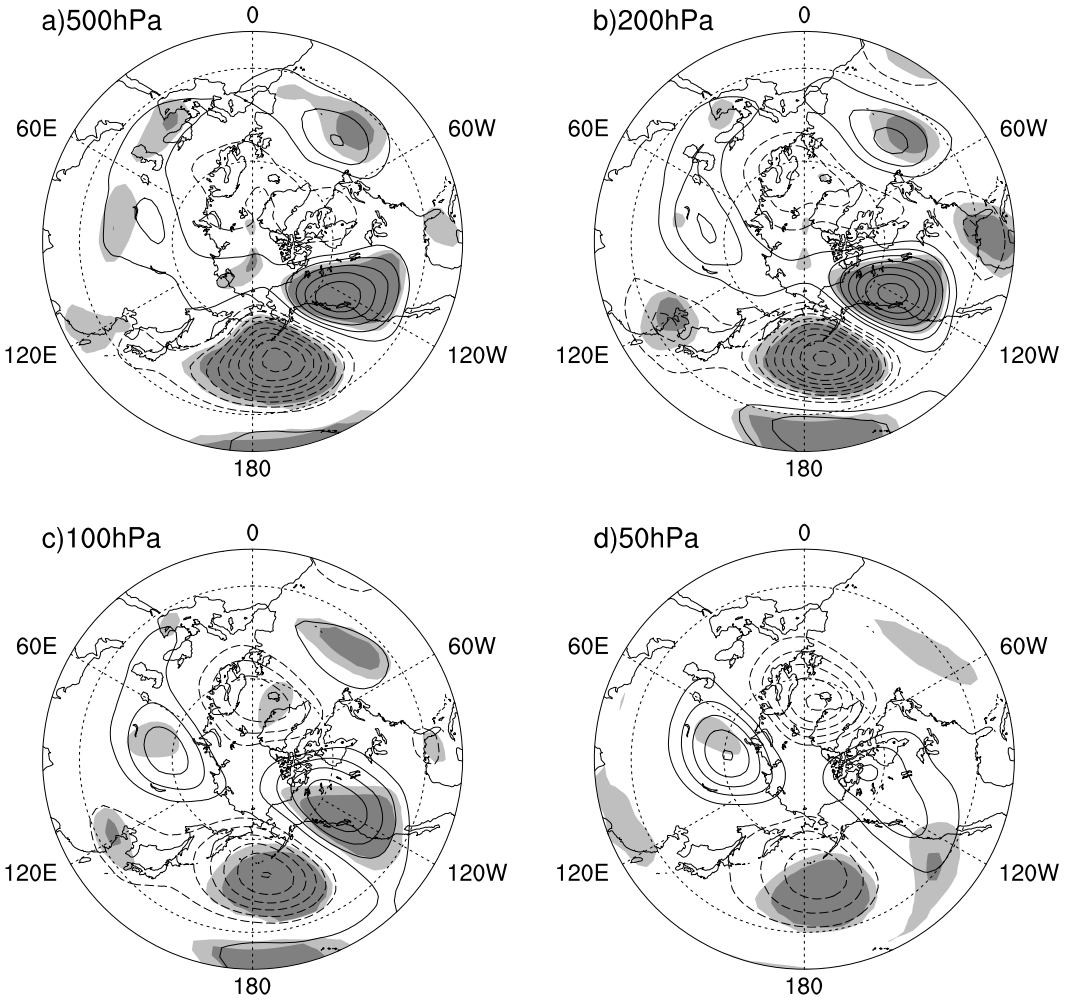

Fig. 5. Difference of the geopotential heights between the active EPW and weak EPW at (a) 500 hPa; (b) 200 hPa; (c) 100 hPa and (d) 50 hPa. Units: $m^2\ s^{-2}$. Contour interval: 200. Solid and dashed lines represent positive and negative values, respectively; zero lines are not shown; light and dark gray shadows show the statistical significance at the 5% level and 1% level, respectively.

sphere and stratosphere. From Fig. 5 we see that this dipole pattern is nearly barotropic and that its two centers both reach the 1% significance level, except the positive center at 50 hPa. A similar anomalous pattern can also be seen in regression maps of the stationary waves upon the EPW index, though the amplitudes are generally weaker in regression maps than in difference maps (not shown). This means that the anomalous pattern associated with the EPW is robust and intrinsic. These results are in agreement with Chen and Wei (2009), Itoh and Harada (2004), and Wang et al. (2007), who studied the stratospheric circulation anomalies associated with the PNA-like events.

The changes in the temperature field associated with the EPW events are shown in Fig. 6. The anomalous patterns revealed in both the difference maps (Fig. 6) and the regression maps (not shown) are highly similar, and the dominant anomalies also occur over North Pacific-North America sector, which again make a PNA-like pattern. But unlike the geopotential height anomalies, which remain in a barotropic state vertically from the troposphere to the lower stratosphere, the temperature anomalies change in sign vertically around 300–250 hPa, where the temperature anomalies are the weakest (not shown). Below 300 hPa the temperature anomalies assume roughly a warm–cool–warm–cool pattern along the North Pacific-North America path, which supports a cool–low and warm–high coupling there between the temperature field and the geopotential height field. Above 250 hPa, the temperature anomalies exhibit roughly a cool–warm–cool–warm pattern, which supports a warm–low and cool–high coupling, leading to the weakening of the geopotential height anomalies there under the constrain of

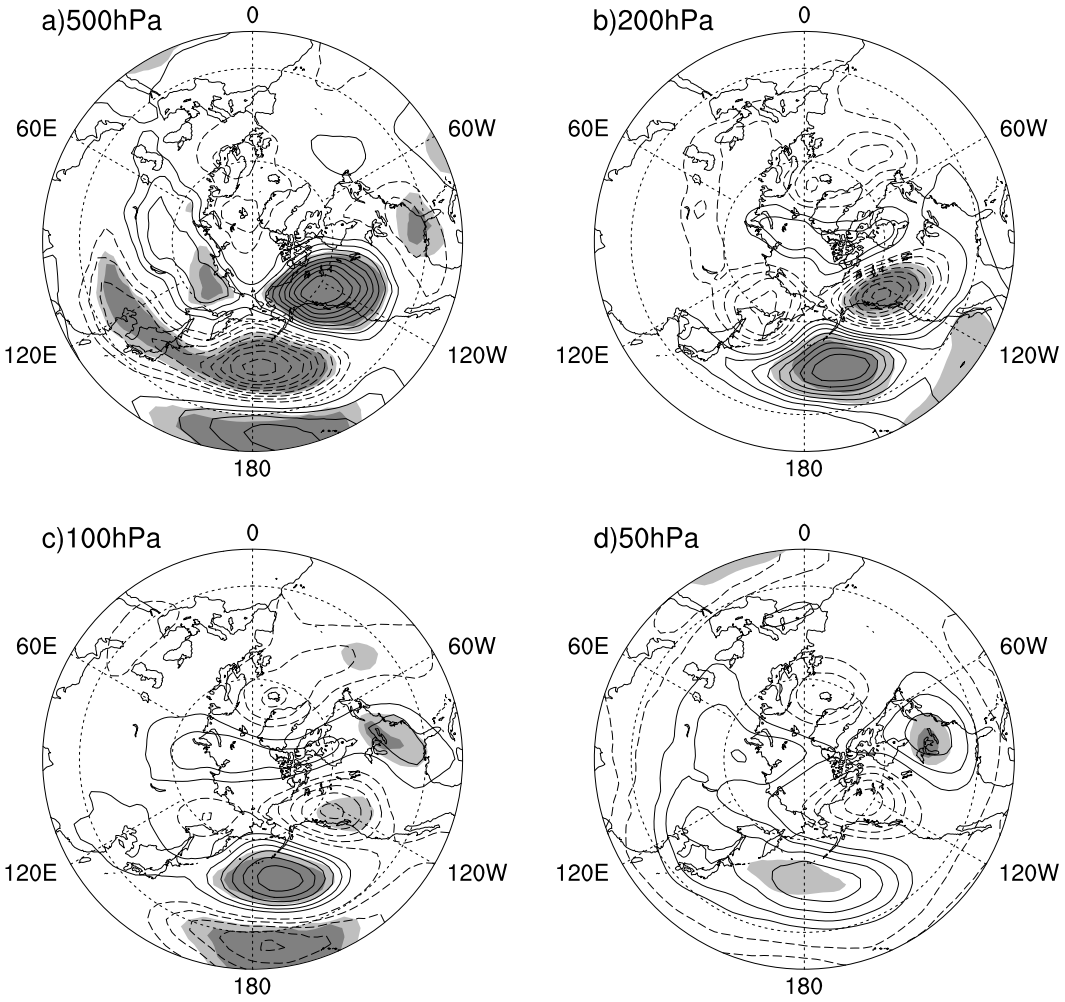

Fig. 6. The same as in Fig. 5, except for the temperature field. Units: K. Contour interval: 0.5. Solid and dashed lines represent positive and negative values, respectively; zero lines are not shown; light and dark gray shadows show the statistically significance at the 5% level and 1% level, respectively.

the thermal wind relation. Notably, the cool anomaly center over the North America in the lower stratosphere at 50 hPa does not reach the 5% significance level.

5. Comparison with the PNA pattern

In this section, we report our detailed comparison of the EPW-related variability with the PNA-related variability to shed light on the linkage of the two phenomena. The geopotential height and temperature anomalous patterns associated with the PNA events were obtained in the same way as for the EPW events. Here, the original definition of the PNA index in Wallace and Gutzler (1981) was used. The results are given in Figs. 7 and 8.

The geopotential height anomalous patterns in the difference (Figs. 5 and 7) and regression maps (not shown) associated with the two phenomena are similar overall, and the average correlation coefficient in the layers 1000 hPa–50 hPa between them reaches as high as 0.87 and 0.95, respectively. Nevertheless, some differences are still noticeable. First, the anomalous North America high behaves differently for the two phenomena. For the EPW events, it is north–south oriented, extending northward across the polar region and joining the anomalous Siberia high, while for the PNA events it is east–west oriented, extending eastward and joining the anomalous North Atlantic high. Secondly, the anomalous low over the southeast United States and the anomalous high over the North Atlantic are slightly stronger for the PNA events than for the EPW events, and they both reached the 1% significance level from the troposphere to the lower strato-

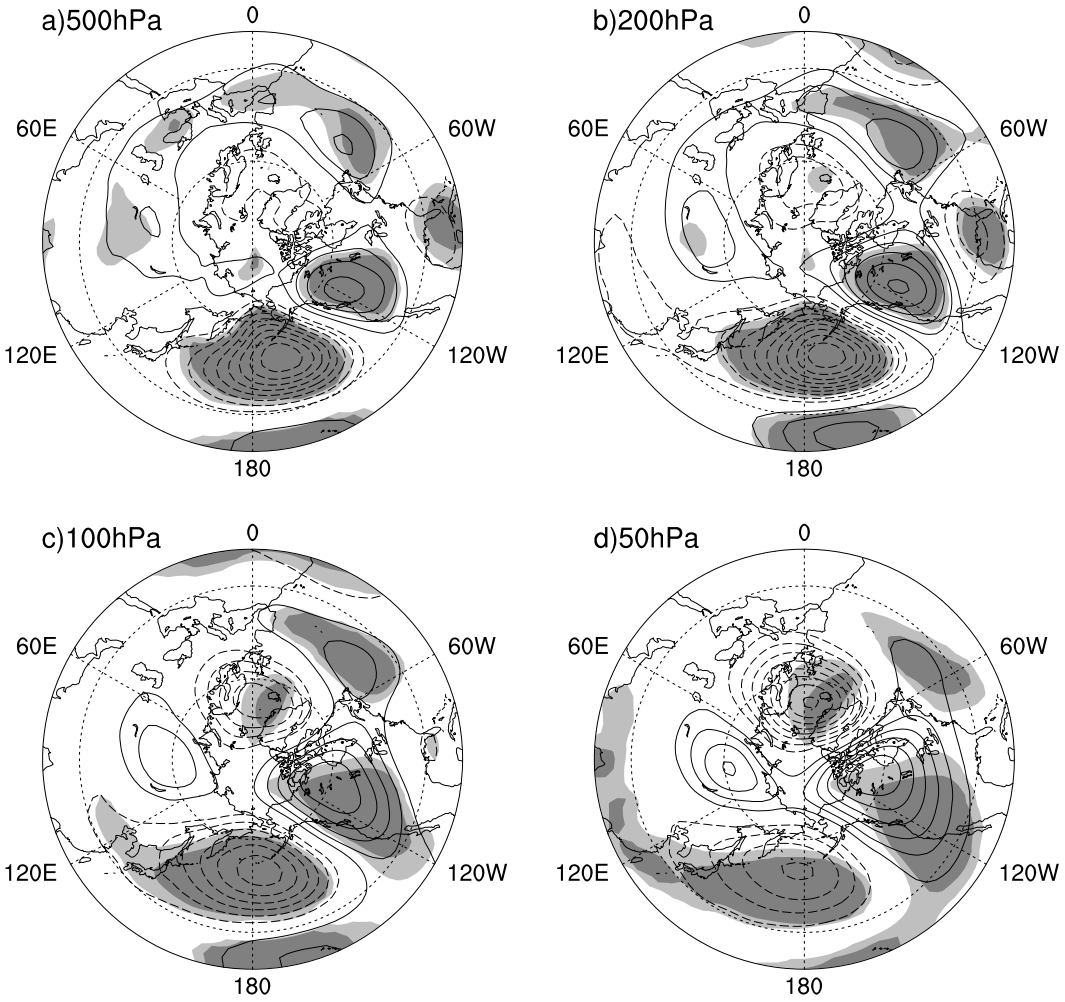

Fig. 7. Difference of the geopotential height of the stationary waves between strong positive PNA and strong negative PNA at (a) 500 hPa; (b) 200 hPa; (c) 100 hPa and (d) 50 hPa. Units: $m^2\ s^{-2}$. Contour interval: 200. Solid and dashed lines represent positive and negative values, respectively; zero lines are not shown; light and dark gray shadows show the statistical significance at the 5% level and the 1% level, respectively.

sphere. Thirdly, the anomalies in the stratosphere are generally much stronger for the PNA events than the EPW events, particularly for the anomalous North America high.

The similar PNA-like patterns of geopotential height anomalies in the troposphere can also be seen in Wang et al. (2007, Fig. 12), which suggests that both the EPW and PNA are likely associated with the ENSO-related SST anomalies. In addition, Chen and Wei (2009) showed that the stratospheric polar vortex variation associated with the ENSO is coupled with a PNA-like wavetrain in the troposphere (Chen and Wei, 2009, their Fig. 10b). In this study we only focused on the relationship between the EPW and PNA, but the influence of ENSO on these two phenomena is a very interesting topic for future research.

The anomalous temperature patterns associated with the EPW and PNA events (Figs. 6 and 8) also show highly similarity, and the average correlation coefficient in the layers 1000 hPa–50 hPa between them reaches as high as 0.81 and 0.84 for the difference (Figs. 6 and 8) and regression maps (not shown), respectively. Nevertheless, some significant differences are still evident. The significant difference is observed over North America, where the anomalous cool center exists at 200 hPa and above for the EPW events, while for the PNA events it disappears except at 200 hPa. As a result of the thermal wind relation, the anomalous North American high is much stronger for the PNA events than the EPW events. Another significant difference can be detected over North Atlantic, where the anomalous North Atlantic cool center in stratosphere

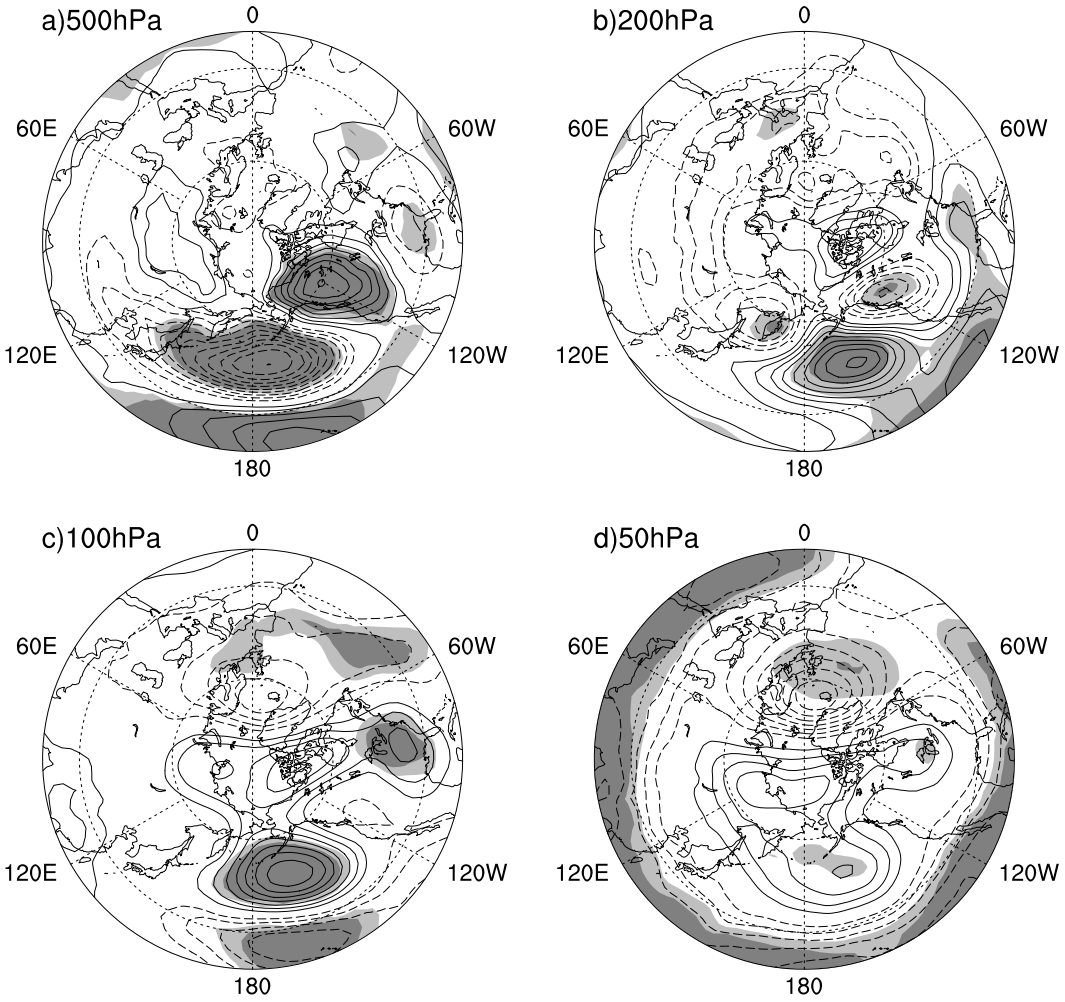

Fig. 8. The same as in Fig. 7, except for the temperature field. Units: K. Contour interval: 0.5. Solid and dashed lines represent positive and negative values, respectively; zero lines are not shown; light and dark gray shadows show the statistically significance at the 5% level and 1% level, respectively.

is much stronger for the PNA events than the EPW events. There is also an interesting difference in the tropics. In both the EPW and PNA events, the cool anomalies cover almost the entire tropics at 50 hPa, but the anomalies in PNA events are ∼1 K cooler and reach the 1% significance level. The reason for this is not clear.

Not only the spatial variability but also the temporal variability of the two phenomena is very similar. The two time series of the EPW and the PNA indices are highly correlated, and the correlation coefficient reaches as high as 0.70 and 0.81 at the 1% confidence level based on the winter mean indices and the 11-year running mean indices, respectively (Fig. 2).

The high similarity between the spatial variation in the geopotential height and the temperature fields of the EPW and the PNA pattern and between the timely evolution of the EPW index and the PNA index strongly suggests that the PNA may very likely be a reflection of the oscillation of the members of the EPW in intensity and position. The difference between the two events should be a result of the different indices used in calculating the related anomalies. The EPW index, which is the averaged vertical stationary wave fluxes in the lower troposphere over the East Pacific, is a good indicator of the vertical propagation of the EPW. While the PNA index, which is the averaged 500-hPa geopotential height of the four action centers of the PNA wavetrain, describes well the horizontal propagation of the EPW in middle troposphere. Generally the horizontal and vertical propagations are closely related, i.e., a strong vertical propagation is accompanied by a strong horizontal propagation; this is the reason that the high degree of similarity is ob-

served. The vertical propagation is of course different from the horizontal propagation, so the existence of the differences between the EPW (viewing from the vertical propagation) and the PNA (viewing from the horizontal propagation) is not surprising.

6. Summary and conclusions

In this study the extensive stationary planetary wave activity over the East Pacific-North America and its variability based on the winter mean have been investigated, and the following conclusions have been reached:

(1) The EPW are evidently detected in northern winters with both ECMWF and NCEP/NCAR reanalyses. The EPW is generated in the lower troposphere over the East Pacific and propagates predominantly downstream into North America and slightly upward into the stratosphere.

(2) The EPW varies in strength from year to year and assumes apparent decadal scale variability. For the period 1958–1964 the EPW is in its second maximum, and it is weakest for the period 1965–1975 while for the period 1976–1987 it is strongest. After 1987 the EPW weakens again.

(3) The members of the EPW, such as the Aleutian low, the East Asian trough, the American trough, and the high in the troposphere, behave differently from winter to winter. For the active EPW, the Aleutian low deepens abnormally and shifts its center from the west to the east of the date line. In the middle and upper troposphere the East Asian trough extends eastward obviously, and the Canadian ridge intensifies abnormally. For the weak EPW, the Aleutian low weakens and shifts its center from east to west of the date line, the East Asian trough retreats back, and the Canadian ridge weakens considerably. The stationary wave members in the lower stratosphere up to 50 hPa also vary in intensity and position for the active versus the weak EPW.

In such a way, the oscillation of the intensity and position of the members of the EPW radiates energy outward in the form of the PNA-like low-frequency oscillation. An active EPW corresponds to a positive PNA, while a weak EPW corresponds to a negative PNA. This process is very similar to radiation from an atom: a radiation is emitting outward when the electronics shift their orbits from one level to another.

Notably, our study dealt with only the propagation features of the EPW and its associated spatial and temporal variability. The mechanisms of the generation and variation of the EPW have not been explored here; we will undertake this investigation in our next study. In addition, it should also be pointed out that the EPW can propagate into the stratosphere. An investigation of how the vertical propagation of the EPW combined with the vertical propagation of the East Asia–West Pacific wavetrain affects the stratosphere–troposphere coupling is currently under way.

Acknowledgements. One of the authors, TAN Benkui, is very grateful to Dr. S. Yang for drawing his attention to Yang and Gutowski (1994)'s work, and to his colleagues Profs. Z. Liu and H. Yang for their comments on the manuscript. This work is supported by the National Natural Science Foundation of China (Grant No. 40533016) and the National Basic Research Program of China (Grant No. 2010CB428606).

REFERENCES

Ambaum, M. H., and B. J. Hoskins, 2002: The NAO troposphere-stratosphere connection. *J. Climate*, **15**, 1969–1978.

Andrews, D. G., and M. E. McIntyre, 1976: Planetary waves in horizontal and vertical shear: The generalized Eliassen-Palm relation and the mean zonal acceleration. *J. Atmos. Sci.*, **33**, 2031–2048.

Andrews, D. G., J. R. Holton, and C. B. Leovy, 1987: *Middle Atmosphere Dynamics*. Academic Press, INC, 504pp.

Baldwin, M. P., and T. J. Dunkerton, 2001: Stratospheric harbingers of anomalous weather regimes. *Science*, **294**, 581–584.

Black, R. X., 2002: Stratospheric forcing of surface climate in the Arctic oscillation. *J. Climate*, **15**, 268–277.

Charney, J. G., and A. Eliassen, 1949: A numerical method for predicting the perturbations of the middle latitude westerlies. *Tellus*, **1**, 38–54.

Charney, J. G., and P. G. Drazin, 1961: Propagation of planetary-scale disturbances from the lower into the upper atmosphere. *J. Geophys. Res.*, **66**, 83–109.

Chen, W., and K. Wei, 2009: Interannual variability of the winter stratospheric polar vortex in the northern hemisphere and their relations to QBO and ENSO. *Adv. Atmos. Sci.*, **26**(5), 855–863, doi: 10.1007/s00376-009-8168-6.

Chen, W., M. Takahashi, and H.-F. Graf, 2003: Interannual variations of stationary planetary wave activity in the northern winter troposphere and stratosphere and their relations to NAM and SST. *J. Geophys. Res.*, **108**, 4797, doi: 10.1029/2003JD003834.

Dickinson, R. E., 1968: Planetary Rossby waves propagating vertically through weak westerly wind wave guides. *J. Atmos. Sci.*, **25**, 984–1002.

Dunkerton, T. J., and M. P. Baldwin, 1991: Quasi-biennial modulation of planetary wave fluxes in the northern hemisphere winter. *J. Atmos. Sci.*, **48**, 1043–1061.

Hartmann, D. L., J. M. Wallace, V. Limpasuvan, D. W.

J. Thompson, and J. R. Holton, 2000: Can ozone depletion and global warming interact to produce rapid climate change? *Proceedings of the National Academy of Sciences of the United States of America*, **97**, 1412–1417.

Haynes, P., 2005: Stratospheric dynamics. *Annual Review of Fluid Mechanics*, **37**, 263–293.

Held, I. M., 1983: Stationary and quasi-stationary eddies in the extratropical troposphere: Theory. *Large-Scale Dynamical Processes in the Atmosphere*, Hoskins and Pearce, Academic Press, 127–168.

Held, I. M., M. Ting, and H. Wang, 2002: Northern winter stationary waves: Theory and modeling. *J. Climate*, **15**, 2125–2144.

Huang, R. H., and K. Gambo, 1982: The response of a hemispheric multilevel model atmosphere to forcing by topography and stationary heat sources. *J. Meteor. Soc. Japan*, **60**, 78–108.

Huang, R. H., and K. Gambo, 1983: On other wave guide in stationary planetary wave propagations in the winter Northern Hemisphere. *Science in China*, **26**, 940–950.

Itoh, H., and K.-I. Harada, 2004: Coupling between troposphere and stratosphere leading modes. *J. Climate*, **17**, 320–336.

Kodera, K., H. Mukougawa, and S. Itoh, 2008: Tropospheric impact of reflected planetary waves from the stratosphere. *Geophys. Res. Lett.*, **35**, L16806, doi: 10.1029/2008GL034575.

Kuroda, Y., and K. Kodera, 1999: Role of planetary waves in the stratosphere-troposphere coupled variability in the northern hemisphere winter. *Geophys. Res. Lett.*, **26**, 2375–2378.

Limpasuvan, V., and D. L. Hartmann, 2000: Wave-maintained annular modes of climate variability. *J. Climate*, **13**, 4414–4429.

Matsuno, T., 1970: Vertical propagation of stationary planetary waves in the winter northern hemisphere. *J. Atmos. Sci.*, **27**, 871–883.

Matsuno, T., 1971: A dynamical model of the stratospheric sudden warming. *J. Atmos. Sci.*, **28**, 1479–1494.

Namias, J., X. Yuan, and D. R. Cayan, 1988: Persistence of North Pacific sea surface temperature and atmospheric flow patterns. *J. Climate*, **1**, 682–703.

Nitta, T., and S. Yamada, 1989: Recent warming of tropic sea surface temperature and its relationship to the Northern Hemisphere circulations. *J. Meteor. Soc. Japan*, **67**, 375–383.

Perlwitz, J., and H.-F. Graf, 2001: Troposphere-stratosphere dynamic coupling under strong and weak polar vortex conditions. *Geophys. Res. Lett.*, **28**, 271–274.

Perlwitz, J., and N. Harnik, 2004: Downward coupling between the stratosphere and troposphere: The relative roles of wave and zonal mean processes. *J. Climate*, **17**, 4902–4909.

Plumb, R. A., 1985: On the three-dimensional propagation of stationary waves. *J. Atmos. Sci.*, **42**, 217–229.

Randel, W. J., and D. L. Williamson, 1990: A comparison of the climate simulated by the NCAR Community Climate Model (CCM1:R15) with ECMWF analyses. *J. Climate*, **3**, 608–633.

Smagorinsky, J., 1953: The dynamical influence of large-scale heat sources and sinks on the quasi-stationary mean motions of the atmosphere. *Quart. J. Roy. Meteor. Soc.*, **79**, 342–366.

Suo, L. L., 2008: Diagnostic study on the mechanisms of the stratosphere polar vortex influencing the troposphere. Ph.D. dissertation, Peking University, 100pp. (in Chinese)

Trenberth, K. E., and J. W. Hurrell, 1994: Decadal atmosphere-ocean variations in the Pacific. *Climate Dyn.*, **9**, 303–309.

Uppala, S. M., and Coauthors, 2005: The ERA-40 reanalysis. *Quart. J. Roy. Meteor. Soc.*, **131**, 2961–3012.

Wallace, J. M., and D. S. Gutzler, 1981: The teleconnection in the geopotential height field during the northern hemisphere winter. *Mon. Wea. Rev.*, **109**, 784–811.

Wallace, J. M., and D. W. J. Thompson, 2002: The Pacific center of action of the northern hemisphere annular mode: Real or artifact? *J. Climate*, **15**, 1987–1991.

Wang, L., W. Chen, and R. Huang, 2007: Changes in the variability of North Pacific Oscillation around 1975/1976 and its relationship with East Asian winter climate. *J. Geophys. Res.*, **112**, D11110, doi: 10.1029/2006JD008054.

Yang, S., and W. J. Gutowski, 1994: GCM simulations of the three-dimensional propagation of stationary waves. *J. Climate*, **7**, 414–433.